

## Multipole-specific, model-independent, velocity-change spectra of collisionally perturbed $^3P_1$ -state $^{174}\text{Yb}$ atoms

A. G. Yodh and T. W. Mossberg

*Department of Physics, Harvard University, Cambridge, Massachusetts 02138*

J. E. Thomas

*Spectroscopy Laboratory and Physics Department, Massachusetts Institute of Technology, Cambridge, Massachusetts 02139*

(Received 6 May 1986)

Coherent transient (echo) techniques have been employed in a high-precision study of collisional velocity thermalization in a sample of  $(6s6p)^3P_1$ , excited-state,  $^{174}\text{Yb}$  atoms perturbed by He or Ar. This work probes the comparative response of aligned and oriented atoms to both depolarizing and to weak, nondepolarizing and/or velocity-changing collisions. By direct inversion of our time-domain echo relaxation data, we also provide a model-independent determination of velocity-change spectra (collision kernels) for nondepolarizing collisions.

The collisional relaxation of magnetically polarized atoms is of fundamental interest, and has been extensively studied. Optical pumping techniques,<sup>1</sup> for example, have been used extensively to elucidate the roles played by qualitatively different types of magnetic order ( $k$  multipoles) in the collisional scattering process, and have provided a wealth of information on *depolarizing* collisions. Depolarizing collisions destroy the internal anisotropy present in the Zeeman manifolds of the colliding species, and thereby play a dominant role in thermalizing the magnetic properties of a given atom. An interesting and different mode of sample relaxation involves the transport of magnetic anisotropies in velocity space.<sup>2</sup> Velocity thermalization of magnetic order occurs when a polarized atom experiences a collision that leaves the atom's internal structure intact, but changes its velocity. To characterize this second relaxation process, one needs to measure complete velocity-change spectra and total cross sections. In the case of weak collisions, access to these quantities has only recently been achieved using photon-echo techniques.<sup>3-6</sup> Significantly, the echo techniques can elucidate the differential relaxation experienced by various  $k$  multipoles in both depolarizing and velocity-changing collision regimes. We note that a variety of laser spectroscopic experiments<sup>7</sup> have explored velocity thermalization in magnetic systems, but for various reasons they could not resolve the effects of the weaker velocity-changing collisions.

In this work, we have employed echo techniques to study the collisional relaxation of *isolated* orientation ( $\rho_0^1$ ) and transverse alignment ( $\rho_2^2$ ) multipoles in the  $(6s6p)^3P_1$ , excited-state, Zeeman manifold of  $^{174}\text{Yb}$  vapor perturbed by He and Ar buffer gases. These measurements have the highest velocity-change resolution of any Zeeman-coherence scattering measurements performed to date, and provide the first comparison of alignment and orientation decay rates sensitive to the effects of both depolarization and deflection. Finally, we have obtained for the first time to our knowledge, *model-independent* scattering kernels (velocity-change spectra) by *direct inversion* of our echo data. Our kernels span the weak diffractive and a portion

of the strong classical collision regime.

Several research efforts<sup>3-5,8</sup> have previously addressed the question of magnetic relaxation in the  $^3P_1$  Zeeman manifold of  $^{174}\text{Yb}$ . Two groups<sup>3,4</sup> measured the collisional relaxation of different combinations of  $k$  multipoles and showed that *populations* ( $\rho_0^0$ ) experienced strong velocity changes in collisions which tended to destroy the *higher multipole moments*. Ghosh, Nabors, Attili, and Thomas<sup>5</sup> concurrently suggested and demonstrated a rather general scheme for the study of certain *isolated* multipole moments that evolve independently in velocity-changing collisions for the cylindrical symmetry appropriate to echo or other laser-type experiments. In the present experiment, we have applied their scheme to compare the relaxation properties of  $\rho_0^1$  and  $\rho_2^2$ .

Our experiment utilizes three polarized, collinear light pulses, all resonant with the  $(6s^2)^1S_0$ - $(6s6p)^3P_1$ ,  $\lambda = 556$  nm transition of  $^{174}\text{Yb}$  to induce a stimulated echo<sup>5,9</sup> [see Figs. 1(a)-1(c)]. Depending on their polarization, the first two laser pulses create orientation ( $\rho_0^1$ ) or transverse alignment ( $\rho_2^2$ ) in the  $^3P_1$  Zeeman manifold with amplitudes that are modulated as a function of axial velocity,  $v_z$  with period  $v_{\text{mod}} \lambda/t_{21}$ . Here  $t_{ij}$  represents the time interval between pulses  $i$  and  $j$ . This variation of  $\rho_0^1$  in velocity space is shown schematically in Fig. 1(d). The third laser pulse generates an echo as a result of its interaction with the velocity modulation in these quantities, and a predetector polarizer selects out only the echo signal arising from the desired multipole moment. These echo signals depend on the persistence of magnetic anisotropy (optical coherences) during  $t_{32}$  ( $t_{e3}$  and  $t_{21}$ ).<sup>9</sup>

We are interested here in the collisional relaxation of magnetic anisotropy<sup>10</sup> during  $t_{32}$ . During this time, *depolarizing* collisions reduce the *magnitude* associated with the various multipole moments, and *velocity-changing* collisions *smooth out the velocity modulation* associated with these moments. Since the echo signal is degraded most strongly by velocity changes larger than  $v_{\text{mod}}$ , by varying  $t_{21}$  one can effectively map out the distribution of velocity changes occurring in a given collisional system. As  $t_{21}$  ap-

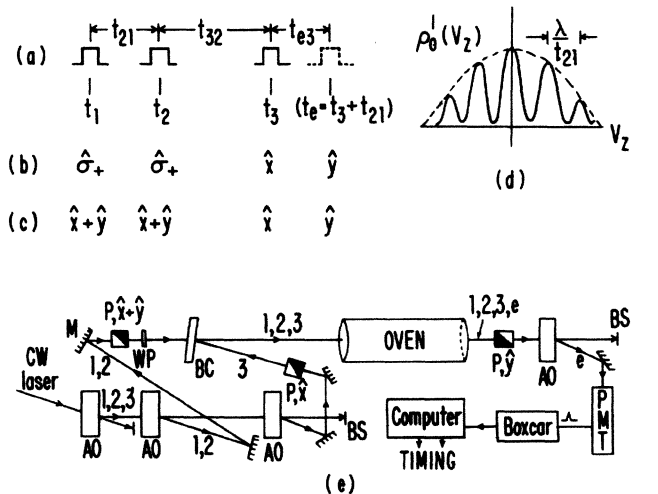


FIG. 1. (a) Excitation-pulse timings. (b) Excitation-pulse polarization directions for orientation ( $\rho_1$ ), and (c) alignment ( $\rho_2$ ). (d) Modulation of  $\rho_1$  in  $v_z$  space introduced through the effects of pulses one and two. The dashed line represents the Doppler velocity distribution. (e) Schematic of apparatus. M, mirrors; BS, beam stop; BC, beam combiner; AO, acousto-optical modulators; P, polarizers (with polarization directions indicated); WP,  $\lambda/4$  wave plate; PMT, photomultiplier tube. The paths of pulses one, two, three, and e (echo) are shown.

proaches zero we recover the pure depolarization rate measured in optical pumping studies.

The collisions discussed above reduce the echo intensity at a rate proportional to a multipole-dependent effective cross section,  $\sigma_{\text{eff}}^{k,q}(t_{21})$ .<sup>3-5,9,11</sup> By measuring echo decay as a function of  $t_{32}$  for various fixed values of perturber pressure and  $t_{21}$ , we have experimentally determined  $\sigma_{\text{eff}}^{k,q}(t_{21})$ . These measurements can be Fourier transformed to yield a multipole-dependent scattering kernel  $W^{k,q}(\Delta v_z)$ , which represents the probability per unit velocity that a single polarization-preserving collision induces an axial velocity change  $\Delta v_z$ .<sup>12</sup> The explicit relation between  $W^{k,q}(\Delta v_z)$  and  $\sigma_{\text{eff}}^{k,q}(t_{21})$  is given below. In deriving this expression we have assumed  $W^{k,q}(\Delta v_z)$  is symmetric about  $\Delta v_z = 0$ .

$$W^{k,q}(\Delta v_z) = \frac{2}{\lambda \sigma_{\text{vcc}}^{k,q}} \int_0^\infty dt_{21} [\sigma_{\text{tot}}^{k,q} - \sigma_{\text{eff}}^{k,q}(t_{21})] \times \cos\left(\frac{2\pi}{\lambda} t_{21} \Delta v_z\right). \quad (1)$$

Here  $\sigma_{\text{tot}}^{k,q} = \sigma_d^{k,q} + \sigma_{\text{vcc}}^{k,q}$  is the total quantum-mechanical scattering cross section, which is equal to the sum of the cross sections for depolarizing ( $\sigma_d^{k,q}$ ) and velocity-changing ( $\sigma_{\text{vcc}}^{k,q}$ ) collisions. In the limit  $t_{21} \rightarrow \infty$ , the difference between total and effective cross sections vanishes.

Our orientation measurements of  $\sigma_{\text{eff}}^{1,0}(t_{21})$  for He-Yb\* and Ar-Yb\* collisions (\* denotes excited-state polarized) are shown in Fig. 2. For both perturbors, the values of  $\sigma_{\text{eff}}^{1,0}$  at large  $t_{21}$  represent the total quantum-mechanical scattering cross section. Similar results were obtained for alignment multipoles. The ratio,  $R(t_{21}) = \sigma^{2,2}(t_{21})/\sigma^{1,0}(t_{21})$ , which is plotted in Fig. 3, elucidates the observed differences in the alignment and orientation cross sections.

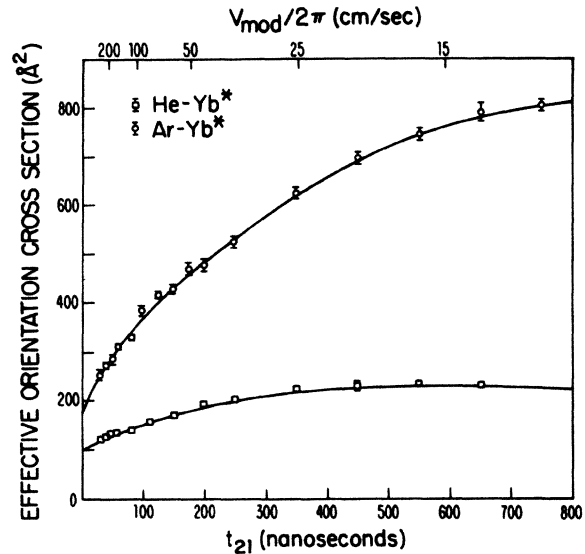


FIG. 2. Measured values of  $\sigma_{\text{eff}}^{1,0}(t_{21})$  as a function of  $t_{21}$  for He-Yb\* and Ar-Yb\* collisions. Each point represents an average of 6–16 separate measurements.

We see that  $R$  is essentially unity for large  $t_{21}$ , demonstrating that the two multipole moments relax identically as the effects of weaker and weaker deflections are included. On the other hand,  $R$  (Yb\*-He) is less than one for small values of  $t_{21}$ . The alignment appears to relax at a rate about 3%–5% lower than the corresponding orientation rate. The cross sections  $\sigma_d^{k,q}$  for orientation and alignment destroying collisions have been calculated<sup>13</sup> using van der Waals scattering potentials and have been found to differ by 12%. Simple extensions of this result to include the effects of velocity-changing collisions sampled at small  $t_{21}$ , indicate that a van der Waals interaction should produce larger differences<sup>3</sup> than we observe.

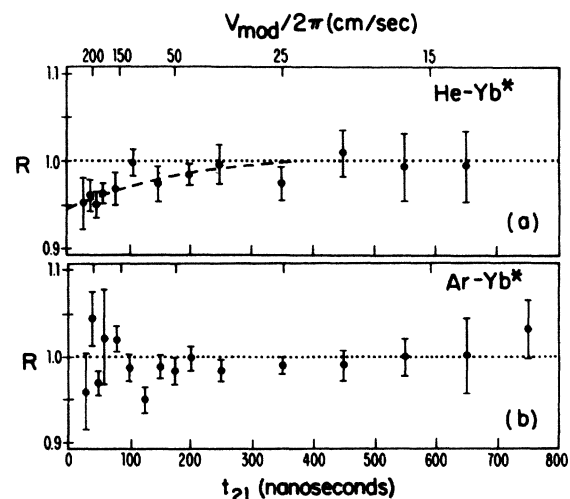


FIG. 3. Ratio of effective alignment collision cross section to orientation collision cross section,  $R$  vs  $t_{21}$  for (a) He-Yb\*, (b) Ar-Yb\* collisions.

*Model-independent* scattering kernels  $W^{1,0}(\Delta v_z)$  were derived from the data in Fig. 2 using Eq. (1). The kernels are plotted in Fig. 4. The kernels exhibit a two-component structure with a narrow central component associated with quantum diffractive collisions, and broad wings associated with small angle classical scattering.<sup>14</sup> Their shapes are not well described by the Gaussian, Lorentzian, or exponential kernels commonly used in theoretical modeling of collisional relaxation. The full width at half maximum of the central component is  $\approx 75$  cm/sec ( $\approx 120$  cm/sec) in the case of Ar-Yb\* (He-Yb\*) and is of the right magnitude to support our identification of the central peak with diffractive velocity changes.<sup>14</sup> By comparing the area in the wings to the area in the central component, we see that classical collisions constitute roughly a quarter of all polarization-preserving collisions. This is quite different from the optical radiator case. Optical coherences have been found to be preserved only in diffractive-type velocity-changing collisions.<sup>15</sup> The difference arises because the Zeeman levels experience similar interaction potentials in all but the very short-range collisional encounters. Our alignment data yielded similar kernels.

In our experiment [see Fig. 1(e)], each of three excitation pulses was generated by gating (with a  $10^6$  on-off ratio) the cw output of an actively stabilized ring dye laser. The pulses, were tuned within  $\approx 100$  MHz of the  $^{174}\text{Yb}$  absorption line center, were typically 20–30 nsec in duration, were collimated to about 1.5 mm in diameter, and had peak powers of 30 mW. The Yb vapor exhibited  $\approx 25\%$  absorption and was housed at  $\approx 390^\circ\text{C}$  in a magnetically shielded oven that had a residual axial field of  $< 18$  mG. Buffer gases were introduced into the oven from a separate reservoir, and their pressures, which varied between 10 and 250  $\mu\text{m}$ , were measured with a capacitance manometer. The experiment was run at 20 kHz, and on every other cycle, pulse one was turned off to provide active baseline subtraction of background noise. Echo signals were averaged with a boxcar integrator, and echo decay was measured in the time domain at fixed pressure. Typically for each value of  $t_{21}$ ,  $t_{32}$  was varied from about 50–800 nsec. Finite perturber pressure echo relaxation data were divided, point by point, by zero-pressure data to yield pure collisional relaxation rates.

We achieved dramatic gains in the precision of this experiment relative to previous ones primarily because of direct computer control of all pulse timings. Echo decay versus  $t_{32}$  was measured by switching (at 40 Hz) between test and reference values of  $t_{32}$  and ratioing the echo intensities. This procedure minimized the effects that laser intensity and frequency fluctuations had on our measurements. Because of the high repetition rate, we could average several hundred echo signals in each 25-msec measurement interval. Differential relaxation between aligned and

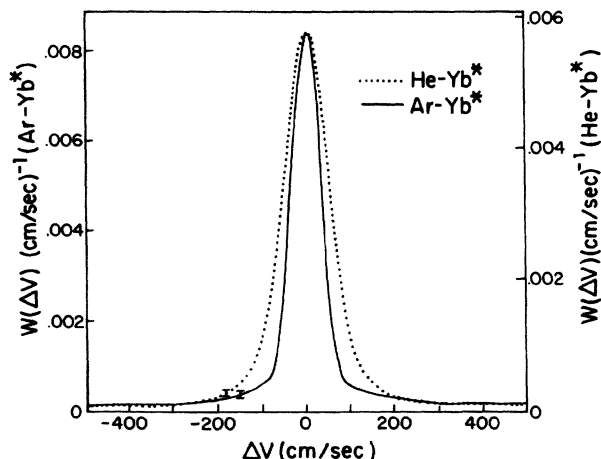


FIG. 4. Velocity-changing collision kernels obtained using Eq. (1) of the text and the data in Fig. 2. The inversions derived from the data in Fig. 2 only provide information concerning collisional velocity changes that are less than  $\approx 350$  cm/sec (because of the minimum values of  $t_{21}$  studied). However, we have used previously measured (Refs. 4 and 5) values of  $\sigma_{\text{eff}}^{1,0}$  at  $t_{21} = 0$  to “reasonably” extend the calculation to  $\Delta v_z > 350$  cm/sec.

oriented samples were measured with high accuracy because it was possible to repeatedly switch from one measurement to another by rotating a quarter-wave retarder [see Fig. 1(e)] while leaving everything else unchanged. The effects of small variations in Yb density, laser tuning, and excitation pulse polarizations were found to be negligible compared to our statistical error.

In conclusion, we have presented a comprehensive set of very high resolution data that demonstrate quantitative differences between He-induced collisional relaxation of alignment ( $\rho_2^2$ ) and orientation ( $\rho_0^1$ ) multipoles in the  $^3P_1$  Zeeman manifold of  $^{174}\text{Yb}$ . Similar systematic differences were not observed for Ar-induced relaxation. Our data were sensitive to differences in the orientation and alignment velocity thermalization rates at the 3% level, and by direct inversion provides the first detailed collisional scattering kernels representative of polarization-preserving collisions. As such, the data represent a substantial advance over previous experimental work.

This research was supported by the National Science Foundation (Grants No. PHY-85-04260 and No. PHY-83-15775), the Joint Services Electronics Program (Contract No. N00014-84-K-0465), and the Department of Defense University Research Instrumentation Program (Contract No. DAAG-29-84-G-0012). One of us (A.G.Y.) gratefully acknowledges financial support from the U.S. Army.

<sup>1</sup>For reviews, see W. Happer, *Rev. Mod. Phys.* **44**, 169 (1972); and A. Omont, *Progress in Quantum Electronics* (Pergamon, London, 1977), Vol. 5, p. 69.

<sup>2</sup>J. L. Le Gouet and P. R. Berman, *Phys. Rev. A* **24**, 1831 (1981).

<sup>3</sup>J. C. Keller and J. L. Le Gouet, *Phys. Rev. A* **32**, 1624 (1985).

<sup>4</sup>A. G. Yodh, J. Golub, and T. W. Mossberg, *Phys. Rev. A* **32**, 844 (1985).

<sup>5</sup>A. P. Ghosh, C. D. Nabors, M. A. Attili, and J. E. Thomas, *Phys. Rev. Lett.* **54**, 1794 (1985); J. E. Thomas, A. P. Ghosh,

- and M. A. Attili, Phys. Rev. A **33**, 3029 (1986).
- <sup>6</sup>J. M. Liang, L. A. Spinelli, R. W. Quinn, R. R. Dasari, M. S. Feld, and J. E. Thomas, Phys. Rev. Lett. **55**, 2684 (1985).
- <sup>7</sup>See, for example, R. Keil, A. Schabert, and P. Toschek, Z. Phys. **261**, 71 (1973); W. K. Bischel and C. K. Rhodes, Phys. Rev. A **14**, 176 (1976); S. N. Atutov, S. G. Rautian, G. D. Rodionov, E. G. Saprykin, and A. M. Shalagin, Opt. Spektrosk. **49**, 1041 (1980) [Opt. Spectrosc. (USSR) **49**, 569 (1980)]; I. Colomb, M. Gorliki, and M. Dumont, Opt. Commun. **21**, 289 (1977); J. Mlynek, Chr. Tamm, E. Buhr, and N. C. Wong, Phys. Rev. Lett. **53**, 1814 (1984).
- <sup>8</sup>See also, I. V. Evseev, V. M. Ermachenko, and V. A. Resehtov, Pis'ma Zh. Eksp. Teor. Fiz. **41**, 132 (1985) [JETP Lett. **41**, 161 (1985)], and references therein.
- <sup>9</sup>T. W. Mossberg and S. R. Hartmann, Phys. Rev. A **23**, 1271 (1981).
- <sup>10</sup>For discussions of spherical tensor multipoles and their relaxation, see K. Blum, *Density Matrix Theory and Applications* (Plenum, New York, 1981); T. Baer, Phys. Rev. A **18**, 2570 (1978).
- <sup>11</sup>The echo intensity decreases as  $I_e(P, t_{32}) = I_0 \exp[-\beta(t_{21}, t_{32})P]$ , where  $P$  is the perturber pressure,  $\beta(t_{21}, t_{32}) = (2n_0/P_0)v_{\text{rel}} t_{32} \sigma_{\text{eff}}^{k,q}(t_{21})$ ,  $n_0$  is the perturber gas number density when the system is at absolute temperature  $T$  and has internal pressure  $P_0$ ,  $v_{\text{rel}} = (8k_B T/\pi\mu)^{1/2}$  is the average echo-atom-perturber-atom relative speed,  $k_B$  is the Boltzmann constant, and  $\mu$  is the echo-atom-perturber-atom reduced mass.
- <sup>12</sup>Since in general  $W^{k,q}(\Delta v_z)$  includes information regarding the phase change incurred in a collision, it need not be positive definite for anisotropic moments and the probability interpretation must be used with caution (see Ref. 5).
- <sup>13</sup>P. R. Berman and W. E. Lamb, Jr., Phys. Rev. **187**, 221 (1969).
- <sup>14</sup>P. R. Berman, in *New Trends in Atomic Physics*, Les Houches Summer School Proceedings, Session 38, edited by G. Grynberg and R. Stora (North-Holland, Amsterdam, 1984).
- <sup>15</sup>R. Kachru, T. J. Chen, S. R. Hartmann, T. W. Mossberg, and P. R. Berman, Phys. Rev. Lett. **47**, 902 (1981); R. A. Forber, L. Spinelli, J. E. Thomas, and M. S. Feld, *ibid.* **50**, 331 (1983).